Eur. Phys. J. Appl. Phys. **42**, 153–159 (2008)
DOI: 10.1051/epjap:2008031

THE EUROPEAN PHYSICAL JOURNAL APPLIED PHYSICS

A constitutive law for magnetostrictive materials and its application to Terfenol-D single and polycrystals

L. Daniel[a] and N. Galopin

Laboratoire de Génie Électrique de Paris, CNRS UMR 8507; SUPELEC; Univ. Paris-Sud; UPMC Univ. Paris 06; 11 rue Joliot-Curie, Plateau de Moulon, 91192 Gif-sur-Yvette Cedex, France

Received: 9 August 2007 / Received in final form 12 October 2007/ Accepted: 18 January 2008
Published online: 28 March 2008 –

Abstract. This paper addresses a multiscale strategy for the prediction of anhysteretic magneto-elastic behavior and its application to the definition of a magneto-elastic constitutive law for Terfenol-D. The multiscale modeling is based on an energetic procedure at the single crystal scale. Localization and homogenization procedures are then applied to deduce the constitutive law of polycrystalline media from the behavior of the corresponding single crystal. The method is applied first to define the magneto-elastic behavior of single crystals, and the application to polycrystalline samples is then considered. Modeling results are compared to experimental data.

PACS. 75.80.+q Magnetomechanical and magnetoelectric effects, magnetostriction – 46.25.Hf Thermoelasticity and electromagnetic elasticity (electroelasticity, magnetoelasticity)

1 Introduction

Magnetostriction is the spontaneous strain that occurs when a magnetic material is subjected to a magnetic field. In the case of rare-earth alloys such as Terfenol-D ($Tb_{0.27}Dy_{0.73}Fe_2$), this strain is far larger (about 10^{-3}) than for most materials, and finds applications in transducer and actuator design [1]. However, the magnetostrictive behavior of Terfenol-D is very sensitive to the application of stress. The prediction of the magneto-elastic behavior of Terfenol-D, including this sensitivity to stress, can lead to optimum design for giant magnetostrictive transducers and actuators. A multiscale strategy for the description of magneto-elastic couplings phenomena has been recently proposed [2,3]. In this approach, a time consuming minimization is necessary to define the single crystal behavior. This minimization procedure can be avoided thanks to the discretization of the single crystal problem. After the presentation of this approach, it is applied to the case of Terfenol-D, firstly by considering single crystals and then polycrystalline media. It must be noticed that the proposed modeling is restricted to reversible (anhysteretic) magneto-elastic behavior.

[a] e-mail: laurent.daniel@lgep.supelec.fr

2 Multi-scale modeling principle

Three distinct scales can be considered in the study of magneto-elastic behavior[1] (Fig. 1):

- the magnetic domains scale (μ);
- the single crystal (or grain) scale (ϕ),;
- the Representative Volume Element (RVE) scale (ℓ).

The modeling principle is based on the description, for each of these scales, of the mechanisms responsible for magneto-elastic couplings.

2.1 Magnetic domain scale

In a magnetic domain, magnetization $\boldsymbol{M}_\alpha$ and magnetostriction $\boldsymbol{\varepsilon}^\mu_\alpha$ are supposed uniform:

$$\boldsymbol{M}_\alpha = M_S\, \boldsymbol{m}_\alpha = M_S\, {}^T[\gamma_1\ \gamma_2\ \gamma_3] \tag{1}$$

$$\boldsymbol{\varepsilon}^\mu_\alpha = \frac{3}{2}\begin{pmatrix} \lambda_{100}(\gamma_1^2-\frac{1}{3}) & \lambda_{111}\gamma_1\gamma_2 & \lambda_{111}\gamma_1\gamma_3 \\ \lambda_{111}\gamma_1\gamma_2 & \lambda_{100}(\gamma_2^2-\frac{1}{3}) & \lambda_{111}\gamma_2\gamma_3 \\ \lambda_{111}\gamma_1\gamma_3 & \lambda_{111}\gamma_2\gamma_3 & \lambda_{100}(\gamma_3^2-\frac{1}{3}) \end{pmatrix}. \tag{2}$$

[1] In most of practical cases, the separation of scales is verified. A notable exception is the grain oriented iron-silicon steels for which magnetic domain size can be of the order of the grain size.

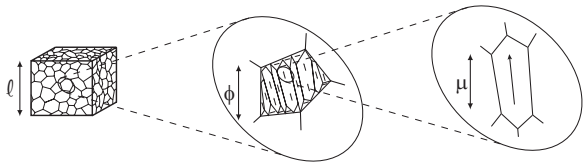

Fig. 1. Scales (polycrystal-grain-domain) for the modeling of magneto-elastic behavior – $\ell \gg \phi \gg \mu$.

Equation (2) is the classical expression for the magnetostriction strain tensor in the case of cubic crystalline symmetry (see for instance [4]). $\boldsymbol{m}_\alpha$ is the direction of the magnetization (unit vector) and $(\gamma_1\ \gamma_2\ \gamma_3)$ its direction cosines, M_S is the saturation magnetization of the material, λ_{100} and λ_{111} its magnetostrictive constants.

The potential energy of a domain is supposed to be the sum of three contributions:

$$W_\alpha = W_\alpha^{mag} + W_\alpha^{an} + W_\alpha^{\sigma}. \tag{3}$$

The expression of these energetic contributions can be written as follows [5]:

– W_α^{mag} is the magneto-static energy, tending to align the magnetization $\boldsymbol{M}_\alpha$ along the magnetic field $\boldsymbol{H}_\alpha$:

$$W_\alpha^{mag} = -\mu_0\, \boldsymbol{H}_\alpha \boldsymbol{M}_\alpha. \tag{4}$$

– W_α^{an} is the magneto-crystalline anisotropy energy tending to prevent the rotation of the magnetization out of the easy axes. This energetic term describes the existence of easy magnetization directions, and thus the existence of domains microstructure:

$$W_\alpha^{an} = K_1(\gamma_1^2\gamma_2^2 + \gamma_2^2\gamma_3^2 + \gamma_3^2\gamma_1^2) + K_2(\gamma_1^2\gamma_2^2\gamma_3^2) \tag{5}$$

K_1 and K_2 denote the anisotropy constants.

– W_α^{σ} is the elastic energy:

$$W_\alpha^{\sigma} = \frac{1}{2}\boldsymbol{\sigma}_\alpha : \boldsymbol{\varepsilon}_\alpha^e \tag{6}$$

$\boldsymbol{\sigma}_\alpha$ and $\boldsymbol{\varepsilon}_\alpha^e$ are respectively the stress and the elastic strain[2] tensors in the domain, linked by the single crystal stiffness tensor $\mathbb{C}_i$ in the usual Hooke law:

$$\boldsymbol{\sigma}_\alpha = \mathbb{C}_i : \boldsymbol{\varepsilon}_\alpha^e. \tag{7}$$

If the magneto-mechanical loading is known, namely the magnetic field $\boldsymbol{H}_\alpha$ and the stress $\boldsymbol{\sigma}_\alpha$, the knowledge of $\boldsymbol{m}_\alpha$ is required to define the magnetization $\boldsymbol{M}_\alpha$ and the magnetostriction strain $\boldsymbol{\varepsilon}_\alpha^\mu$ in the considered magnetic domain.

2.2 Single crystal scale

A single crystal (or grain) is defined as a zone where elastic properties are uniform (stiffness tensor $\mathbb{C}_i$). From the magnetic point of view, the crystal is divided into domain families, each corresponding to a particular direction of the magnetization. For any possible magnetization direction $\boldsymbol{m}_\alpha$, the lower the potential energy W_α, the higher the existence probability. The existence probability f_α of a magnetization direction $\boldsymbol{m}_\alpha$ in a single crystal is defined thanks to a Boltzmann explicit relation [2,6] given by equation (8)

$$f_\alpha = \frac{\exp(-A_s.W_\alpha)}{\displaystyle\int_\alpha \exp(-A_s.W_\alpha)} \tag{8}$$

A_s is an additional modeling parameter. It has been shown [3] to be proportional to the initial slope of the anhysteretic magnetic curve when no stress is applied. The identification of A_s can be made using one magnetic curve. All the other parameters are classical physical constants of the material, identified with independent experimentations.

Once the existence probability for each direction $\boldsymbol{m}_\alpha$ is known, magnetization $\boldsymbol{M}_i$ and magnetostriction $\boldsymbol{\varepsilon}_i^\mu$ in the single crystal are obtained thanks to an averaging operation over all possible directions:

$$\boldsymbol{M}_i = \langle \boldsymbol{M}_\alpha \rangle = \int_\alpha f_\alpha\, \boldsymbol{M}_\alpha \tag{9}$$

$$\boldsymbol{\varepsilon}_i^\mu = \langle \boldsymbol{\varepsilon}_\alpha^\mu \rangle = \int_\alpha f_\alpha\, \boldsymbol{\varepsilon}_\alpha^\mu. \tag{10}$$

From a practical point of view, this integral is evaluated numerically after discretization of the directions $\boldsymbol{m}_\alpha$ in space. The possible directions for $\boldsymbol{m}_\alpha$ are described through the mesh of a unit radius sphere S (N unit vectors $\boldsymbol{x}_n$ with components x_{ni}, $i = 1, 2, 3$). We used a 10242 point mesh. The — approximative — isotropy of the mesh is verified to avoid mesh anisotropy effects in the proposed modeling. For that purpose, the values given in Table 1 are compared to their theoretical value.

The size of the mesh is chosen to ensure a sufficiently small difference between discrete and numerical values. Using such a mesh, equations (8), (9) and (10) can be discretized, and the — time consuming — minimization of the potential energy (proposed in [2,3] in order to determine the direction of magnetization in the magnetic domains) is not required. Indeed the directions corresponding to high (resp. low) energy levels will be associated to low (resp. high) existence probability in equation (8).

2.3 Representative volume element scale

The Representative Volume Element (RVE), or macroscopic scale, is the scale at which the constitutive law is written, and at which the applied solicitations (magnetic field and stress) are known. It is a zone large enough so that its magneto-elastic behavior is representative for the whole material behavior. Since the material is heterogeneous, localization-homogenization rules, depending on

[2] The relationship between the elastic strain and the magnetostriction strain is not trivial, and can be estimated using appropriate localization-homogenization procedures [3].

Table 1. Verification of the mesh isotropy – $N = 10242$, $i = 1, 2, 3$, $j = 1, 2, 3$.

Discrete integral Di	Reference integral Ri	$\lvert Ri - Di\rvert$
$\frac{1}{N}\sum_{n=1}^{N} x_{ni}$	$\frac{1}{4\pi}\iint_S \gamma_i dS$	$<10^{-16}$
$\frac{1}{N}\sum_{n=1}^{N} x_{ni}^2$	$\frac{1}{4\pi}\iint_S \gamma_i^2 dS$	$<10^{-8}$
$\frac{1}{N}\sum_{n=1}^{N} x_{ni}x_{nj},\ i \neq j$	$\frac{1}{4\pi}\iint_S \gamma_i\gamma_j dS,\ i \neq j$	$< 10^{-9}$
$\frac{1}{N}\sum_{n=1}^{N} x_{ni}^3$	$\frac{1}{4\pi}\iint_S \gamma_i^3 dS$	$<2 \times 10^{-16}$
$\frac{1}{N}\sum_{n=1}^{N} x_{n1}x_{n2}x_{n3}$	$\frac{1}{4\pi}\iint_S \gamma_1\gamma_2\gamma_3 dS$	$< 10^{-17}$
$\frac{1}{N}\sum_{n=1}^{N} x_{ni}^4$	$\frac{1}{4\pi}\iint_S \gamma_i^4 dS$	$<2 \times 10^{-8}$
$\frac{1}{N}\sum_{n=1}^{N} x_{ni}^2x_{nj}^2,\ i \neq j$	$\frac{1}{4\pi}\iint_S \gamma_i^2\gamma_j^2 dS,\ i \neq j$	$<2 \times 10^{-8}$
$\frac{1}{N}\sum_{n=1}^{N} x_{ni}^6$	$\frac{1}{4\pi}\iint_S \gamma_i^6 dS$	$<2 \times 10^{-4}$
$\frac{1}{N}\sum_{n=1}^{N} x_{n1}^2x_{n2}^2x_{n3}^2$	$\frac{1}{4\pi}\iint_S \gamma_1^2\gamma_2^2\gamma_3^2 dS$	$<10^{-4}$

the microstructure, are necessary to deduce the local loadings from the macroscopic ones. In the proposed modeling, a self-consistent scheme is used [3].

The local magnetic field $\boldsymbol{H}_i$ is deduced from the macroscopic magnetic field $\boldsymbol{H}_m$ according to equation (11) deduced from the resolution of an inclusion problem[3].

$$\boldsymbol{H}_i = \frac{3 + 3\chi_m}{3 + \chi_i + 2\chi_m}\boldsymbol{H}_m \tag{11}$$

χ_m and χ_i are respectively the magnetic susceptibility of the polycrystal and of the single crystal. Since the magnetic behavior is usually non-linear, a secant definition is used:

$$\chi_m = \frac{||\boldsymbol{M}_m||}{||\boldsymbol{H}_m||} \qquad \chi_i = \frac{||\boldsymbol{M}_i||}{||\boldsymbol{H}_i||}. \tag{12}$$

The local stress tensor $\boldsymbol{\sigma}_i$ is deduced from the macroscopic stress tensor $\boldsymbol{\sigma}_m$ according to equation (13).

$$\boldsymbol{\sigma}_i = \mathbb{B} : \boldsymbol{\sigma}_m. \tag{13}$$

The fourth order tensor $\mathbb{B}$ is the so-called stress concentration tensor. In the self-consistent case, the tensor $\mathbb{B}$ can be calculated according to equation (14).

$$\mathbb{B} = \mathbb{C}_i : (\mathbb{C}_i + \mathbb{C}^*)^{-1} : (\mathbb{C}_m + \mathbb{C}^*) : {\mathbb{C}_m}^{-1} \tag{14}$$

[3] Inclusion based models rely on the hypothesis that mean fields in each phase i are similar to corresponding fields of an inclusion of phase i embedded in an infinite homogeneous medium with magnetic property χ_m [7]. In the self-consistent case, χ_m is the magnetic susceptibility of the polycrystal.

$\mathbb{C}_m$ is the stiffness tensor of the polycrystal and $\mathbb{C}^*$ is the Hill constraint tensor deduced from the resolution of the Eshelby's inclusion problem (see for example [8]). Once the local loading is known, the local modeling can be applied. The macroscopic response (macroscopic magnetization $\boldsymbol{M}_m$ and macroscopic magnetostriction strain $\boldsymbol{\varepsilon}_m^{\mu}$) is then deduced thanks to a classical homogenization step, according to equations (15) and (16).

$$\boldsymbol{M}_m = \langle \boldsymbol{M}_i \rangle \tag{15}$$

$$\boldsymbol{\varepsilon}_m^{\mu} = \langle {}^t\mathbb{B} : \boldsymbol{\varepsilon}_i^{\mu} \rangle. \tag{16}$$

Since the single crystal is usually anisotropic, the knowledge of the crystallographic texture of the polycrystal is required. The crystallographic texture can be described through an Orientation Distribution Function (ODF), representative of the orientations of grains in the polycrystal [9]. A Scanning Electron Microscope (SEM), with an Electron Back Scatter Diffraction (EBSD) measurement system, can provide a discrete Orientation Data File for the crystallographic texture of a given material.

2.4 Summary of the multiscale scheme

The principle of the multiscale modeling is summarized on Figure 2. Entry data are material parameters for the single crystal (elastic, magnetic and magnetostrictive constants), texture data and A_s parameter for the polycrystal, and the macroscopic magneto-mechanical loading. Since the localization procedure requires an estimation of macroscopic magnetization and strain, an initial solution is also needed. This initial solution can be arbitrarily chosen, but the closest to the solution, the faster the convergence of the calculation. The hypotheses of uniform magnetic field and stress within the polycrystal can be used for the definition of that initial solution. The classical multiscale scheme is then performed until convergence, including the localization step, the local constitutive law application and the homogenization step.

3 Application to Terfenol-D single crystals

The multiscale modeling is applied first to Terfenol-D single crystals for which experimental results can be found in the literature. The material properties of the Terfenol-D single crystal have also been collected in the literature. They are summarized in Table 2. Both magnetic and magnetostrictive properties have been investigated. The value of the parameter A_s has been taken to 2×10^{-3} m^3/J.

3.1 Magnetic behavior

In order to exhibit the anisotropy of the magnetic behavior, the M-H curves have been plotted for a magnetic field applied in three directions of the single crystal, namely

Table 2. Terfenol-D properties: Saturation magnetization, anisotropy, magnetostrictive and elastic constants.

Constant	M_S	(K_1, K_2)	$(\lambda_{100}, \lambda_{111})$	(C_{11}, C_{12}, C_{44})
Value	8 10^5 A/m	$(-0.8, -1.8)$ 10^5 J/m^3	$(9, 164)$ 10^{-5}	$(141, 65, 49)$ GPa
Reference	[10]	[1]	[11]	[12]

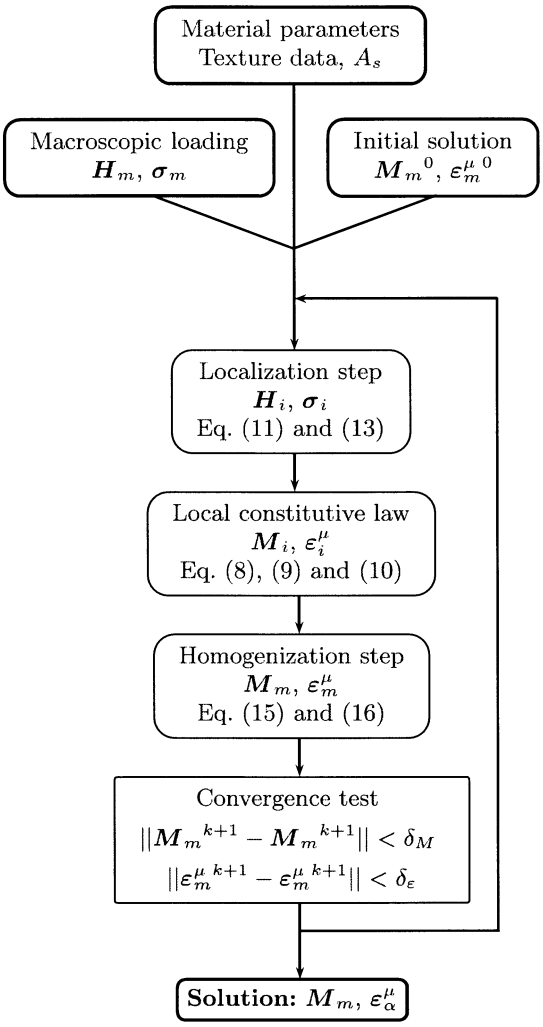

Fig. 2. Multiscale scheme: principle.

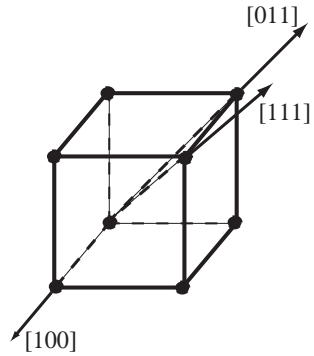

Fig. 3. Crystallographic frame in the cubic symmetry.

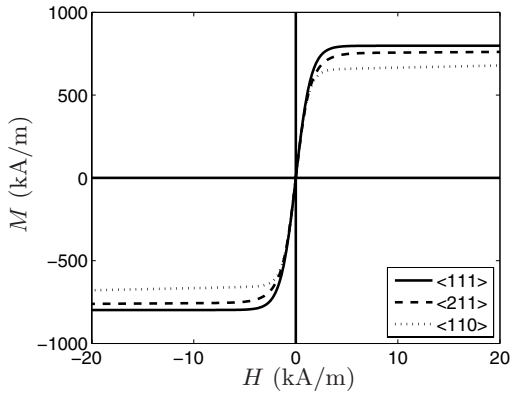

Fig. 4. Predicted anhysteretic magnetic behavior in different crystallographic directions for Terfenol-D single crystal in the stress-free case.

$\langle 111 \rangle$, $\langle 211 \rangle$ and $\langle 110 \rangle$ direction. These directions are defined with respect to the crystallographic frame (Fig. 3).

The modeling results are plotted in Figure 4.

The relative anisotropy of the single crystal is in good agreement with the results reported by Wang et al. [13]. The best magnetization directions are the $\langle 111 \rangle$ directions. However, the magnetic field levels do not correspond to those obtained experimentally. The value of the magnetic field H is defined in the simulation as the mean value of the magnetic field over the material. Concerning the experimental results, this value is difficult to define precisely and is often calculated from the value of the current intensity in the windings used to create the magnetic field. Such a calculation usually neglects the strong macroscopic demagnetizing field effects involved in such experimental apparatus. This point could explain the discrepancies between the magnetic field levels in experimental and numerical results. Unfortunately, data concerning the evaluation of the magnetic field are usually not given in the corresponding experimental papers.

3.2 Magnetostrictive behavior

The magnetostrictive behavior has also been evaluated. The magnetostriction curves have been plotted for a magnetic field applied in different directions of the single crystal. The results are plotted in Figure 5.

Here again, the predicted relative anisotropy is in good agreement with the results reported in [13], but the magnetic field axes do still not correspond, probably due to demagnetizing field effects.

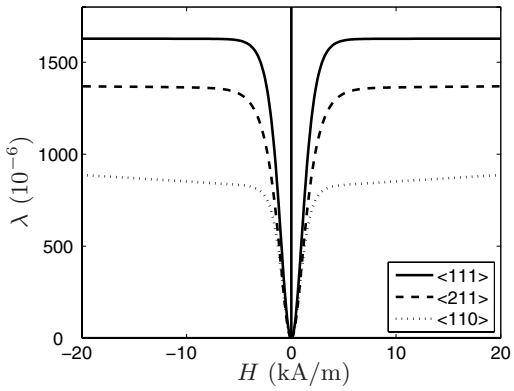

Fig. 5. Predicted anhysteretic magnetostrictive behavior in different crystallographic directions for Terfenol-D single crystal in the stress-free case.

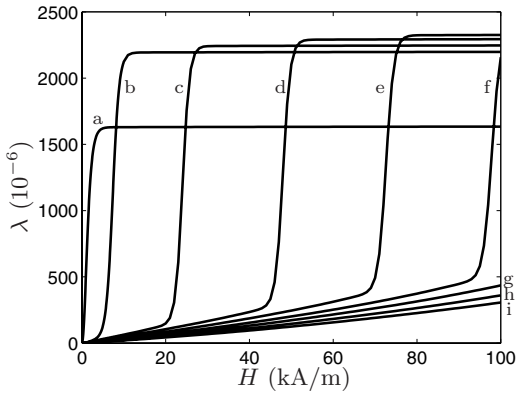

Fig. 6. Predicted anhysteretic magnetostrictive behavior of Terfenol-D single crystal: effect of a compression stress along a ⟨111⟩ direction (a:0, b:2, c:7, d:14, e:21, f:28, g:34, h:41, i:48 MPa).

3.3 Magnetostriction under stress

The magnetostriction strain is known to be dependent on stress. The ε^{μ}-H curves have been plotted for different levels of compressive stress. Both stress and magnetic field are applied along a ⟨111⟩ direction. The results are plotted in Figure 6.

Two tendencies are observed. For low magnetic field levels, the application of a stress tends to decrease the magnetostriction amplitude. On the other hand, the saturation magnetostriction strain is increasing with the applied stress. This latter effect is sensitive for low applied stress but saturates for higher levels. As a consequence, the magnetostriction curves are crossing each others. Such an effect has been observed experimentally by Clark et al. [14]. Unfortunately, a quantitative comparison is not possible because of the unknown definition of the magnetic field in the experimental data. Moreover, a small disorientation angle of the magnetic field (or stress) from the ⟨111⟩ direction can significantly modify the results, both experimental and numerical.

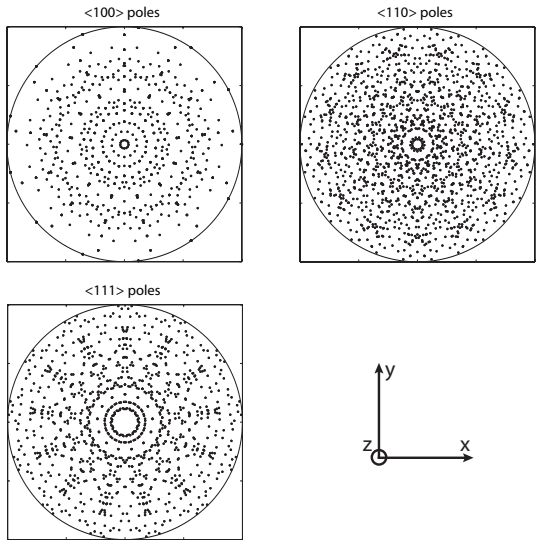

Fig. 7. Pole figures for an isotropic polycrystal obtained by regular zoning of the crystallographic orientations space (stereographic projection).

However, the single crystal modeling has been shown to capture the main magneto-elastic properties, at least qualitatively. We can apply the proposed constitutive law to a polycrystalline specimen.

4 Application to polycrystalline Terfenol-D

In most applications, Terfenol-D is used in its polycrystalline form. A polycrystal can be seen as a crystallite aggregate. The only additional data needed for the modeling are the crystallites orientation. These orientations are given by an Orientation Distribution Function. This ODF can be represented in stereographic projection on a pole figure (see for instance [9]). In the case of an isotropic polycrystalline Terfenol-D sample, the crystallites orientation is random. The crystallographic texture represented by the discrete pole figure of Figure 7 can be used to describe such an isotropic behavior [3].

The results obtained for the magnetostriction strain as a function of the magnetic field for several levels of stress are presented in Figure 8.

The same kind of effect than for the single crystal is observed: for a given level of magnetic field, the application of a compressive stress tends first to increase the magnetostriction strain and then to decrease it. It is consistent with the existence of an optimal pre-load stress for magnetostrictive actuators. The qualitative evolution of the magnetostriction with respect to stress is in agreement with experimental results previously reported in the literature [1,15] or by giant magnetostrictive material manufacturers [16]. Since a quantitative comparison is difficult unless the precise experimental conditions are known, particularly for the magnetic field level definition, a specific experimental setup has been developed [17]. Anhysteretic measurements have been performed on a 10 mm diameter Terfenol-D rod. The sample is placed in

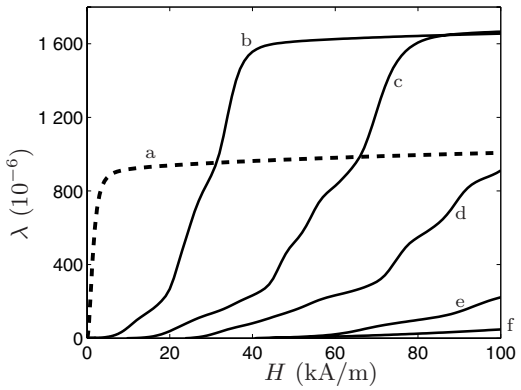

Fig. 8. Predicted anhysteretic magnetostrictive behavior of Terfenol-D polycrystal: effect of a compression stress along the magnetization direction (a:0, b:10, c:20, d:30, e:50, f:80 MPa).

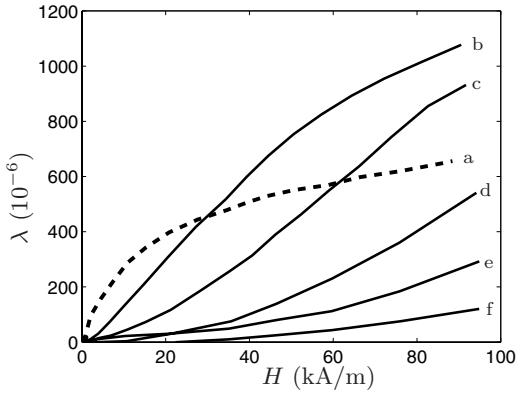

Fig. 9. Experimental anhysteretic magnetostrictive behavior of Terfenol-D polycrystal: effect of a compression stress along the magnetisation direction (a:0, b:10, c:20, d:30, e:50, f:80 MPa).

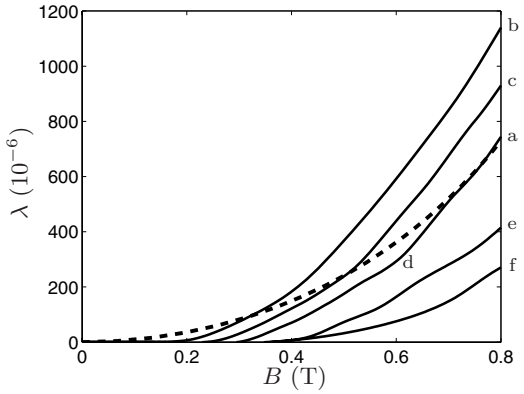

Fig. 10. Predicted anhysteretic magnetostrictive behavior of Terfenol-D polycrystal: effect of a compression stress along the magnetization direction (a:0, b:10, c:20, d:30, e:50, f:80 MPa).

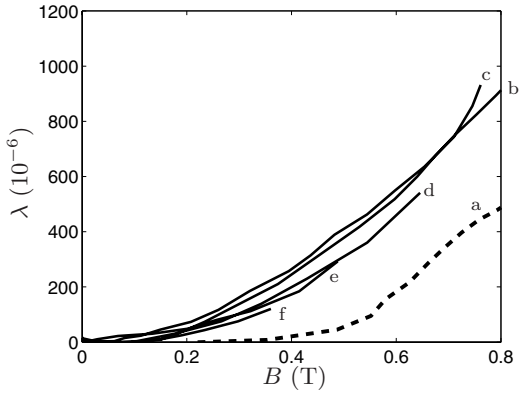

Fig. 11. Experimental anhysteretic magnetostrictive behavior of Terfenol-D polycrystal: effect of a compression stress along the magnetization direction (a:0, b:10, c:20, d:30, e:50, f:80 MPa).

a tension-compression test machine equipped with a magnetic solicitation apparatus. Stress and strain are respectively measured thanks to a standard load cell and strain gages. The applied magnetic field is measured thanks to Hall effect sensors, and the magnetic induction B in the sample is obtained through the integration of the induced voltage on a B-coil surrounding the specimen. The results are presented in Figure 9.

Except for the maximum strain level that is over-estimated by the model, the agreement is satisfying. Indeed, it must be recalled that the proposed multiscale approach does not use the modeled curves for any adjustment operation. The material parameters are taken from the literature (see Tab. 2).

The magnetostriction strain is often written as a function of the magnetic induction $\boldsymbol{B}$. The corresponding curves are plotted in Figure 10, assuming that the material is isotropic, so that the magnetic induction $\boldsymbol{B}$, the magnetic field $\boldsymbol{H}$ and the magnetisation $\boldsymbol{M}$ are parallel (and then $B = \mu_0(H + M)$).

The corresponding experimental data is plotted in Figure 11.

Both modeling and experimental results show that the magnetostriction strain first increase for low applied stress and then decrease. But this decrease is very significant according to the model whereas experiments shows that the compressive stress, after a minimal pre-load, has no strong influence on the $B(H)$ curve. This is in accordance with an usual hypothesis for macroscopic magnetostriction strain modeling of Terfenol-D (see for instance [18]) assuming that the $\lambda(B)$ curve is not stress-dependent. However, it seems to be very particular to Terfenol-D, for which the effect of stress on magnetostriction saturates very early, and should not be taken as a general property.

5 Conclusion

A multiscale approach for magnetostrictive behavior modeling has been presented. It is based on a statistical energetic description of the domain microstructure evolution. This approach has been applied to Terfenol-D single crystals and polycrystals. It has been shown to capture the

main features of this material's behavior. One of the objective of such an approach would be to replace experiments for the identification of macroscopic models used in numerical simulation for the design of electromagnetic devices. However this approach is limited to anhysteretic behavior. The extension to hysteretic behavior is necessary and supposes to modify the formulation in an incremental way. It can be done by using the variation of the existence probability of a given magnetization direction δf_α instead of f_α in the model. The definition of δf_α is given by differentiation of equation (8):

$$\delta f_\alpha = \frac{e^{-A_s.W_\alpha} - \int_\alpha e^{-A_s.W_\alpha}}{\int_\alpha e^{-A_s.W_\alpha}} A_s\, f_\alpha\, \delta W_\alpha. \qquad (17)$$

This extension is presently a work in progress and will lead to a full magneto-elastic modeling including hysteresis.

References

1. G. Engdahl, *Handbook of Giant Magnetostrictive Materials* (Academic Press, 2000)
2. N. Buiron, L. Hirsinger, R. Billardon, J. Phys. IV France **9**, 187 (1999)
3. L. Daniel, N. Buiron, O. Hubert, R. Billardon, J. Mech. Phys. Solids, in press, available on-line: doi:10.1016/j.jmps.2007.06.003
4. E. du Trémolet de Lacheisseirie, *Magnetostriction — Theory and applications of magnetoelasticity* (CRC Press, 1993)
5. A. Hubert, R. Schäfer, *Magnetic domains* (Springer, 1998)
6. S. Chikazumi, *Physics of Ferromagnetism*, 2nd edn. (Clarendon Press, 1997)
7. L. Daniel, R. Corcolle, IEEE Trans. Magn. **43**, 3153 (2007)
8. M. Bornert, T. Bretheau, P. Gilormini, *Homogenization in Mechanics of Materials* (ISTE Publishing Company, 2007)
9. H.J. Bunge, *Texture Analysis in Materials Science* (Butterworths, 1982)
10. L. Sandlund, M. Fahlander, T. Cedell, A.E. Clark, J.B. Restorff, M. Wun-Fogle, *Proc. 4th Conf. New Actuators* (Bremen, Germany, 1994), pp. 210–213
11. D.C. Jiles, *Introduction to Magnetism and Magnetic Materials* (Chapman & Hall, 1991)
12. A.E. Clark, in *Ferromagnetic Materials*, edited by E.P. Wohlfarth (North-Holland Publishing Company, 1980)
13. B.W. Wang, S.C. Busbridge, Y.X. Li, G.H. Wu, A.R. Piercy, J. Magn. Magn. Mater. **218**, 198 (2000)
14. A.E. Clark, H.T. Savage, M.L. Spano, IEEE Trans. Magn. **20**, 1443 (1984)
15. M. Wun-Fogle, J.B. Restorff, K. Leung, J.R. Cullen, A.E. Clark, IEEE Trans. Magn. **35**, 3817 (1999)
16. Etrema - Terfenol-D Data Sheet. http://etrema-usa.com/documents/Terfenol.pdf
17. N. Galopin, L. Daniel, F. Bouillault, M. Besbes, Przegląd Elektrotechnic. **6**, 44 (2007)
18. K. Azoum, M. Besbes, F. Bouillault, T. Ueno, Eur. Phys. J. Appl. Phys. **36**, 43 (2006)